forests

MDPI

Article

Impact of Root Rot Disease of *Zanthoxylum armatum* on Rhizosphere Soil Microbes and Screening of Antagonistic Bacteria

Shan Han [1,2,3,†], Zhenlei Zheng [1,†], Shujiang Li [1,2,3], Yinggao Liu [1,2,3], Shuying Li [1,2,3], Chunlin Yang [1,2,3], Tianmin Qiao [1], Tiantian Lin [1,*] and Tianhui Zhu [1,2,3,*]

[1] College of Forestry, Sichuan Agricultural University, Chengdu 611130, China; 13722@sicau.edu.cn (S.H.); 2020204017@stu.sicau.edu.cn (Z.Z.); 14087@sicau.edu.cn (S.L.); 11468@sicau.edu.cn (Y.L.); 72111@sicau.edu.cn (S.L.); yangcl0121@163.com (C.Y.); 11470@sicau.edu.cn (T.Q.)
[2] Key Laboratory of Forest Protection of Sichuan Education Department, Chengdu 611130, China
[3] Key Laboratory of National Forestry & Grassland Administration on Forest Resources Conservation and Ecological Safety in the Upper Reaches of the Yangtze River, Chengdu 611130, China
* Correspondence: tlin@sicau.edu.cn (T.L.); 10627@sicau.edu.cn (T.Z.)
† These authors contributed equally to this work.

Abstract: *Zanthoxylum armatum*, a significant forest plant in southwestern China, is crucial for preserving soil and water resources. However, the presence of root rot disease has led to plant death, impacting the pepper sector. Effective control measures for this disease are still lacking. Rhizosphere microorganisms play a vital role in plant health by inhibiting plant pathogens and inducing plant resistance. This research aimed to isolate and characterize the pathogen responsible for root rot disease in *Z. armatum*. Comparative analysis of fungal and bacterial communities in the rhizosphere soil of healthy and diseased plants revealed *Fusarium solani* as the pathogenic fungus causing root rot disease. Diseased plants had a higher occurrence of *Fusarium* spp., while disease-free plants had a higher abundance of ecologically beneficial microbial communities that could potentially serve as biocontrol agents. Three bacterial strains (*Bacillus subtilis*, *Bacillus amyloliquefaciens*, and *Bacillus siamensis*) were identified as effective biocontrol agents, inhibiting the growth of the pathogenic fungus *F. solani* both in vivo and in vitro. This study deepens our understanding of the rhizosphere soil microbial community differences between diseased and healthy *Z. armatum*, providing potential biocontrol bacteria to enhance plant resistance against root rot disease.

Keywords: root rot disease; plant-microbe interactions; pathogen resistance; microbiome assemblage

Citation: Han, S.; Zheng, Z.; Li, S.; Liu, Y.; Li, S.; Yang, C.; Qiao, T.; Lin, T.; Zhu, T. Impact of Root Rot Disease of *Zanthoxylum armatum* on Rhizosphere Soil Microbes and Screening of Antagonistic Bacteria. *Forests* **2023**, *14*, 1561. https://doi.org/10.3390/f14081561

Academic Editor: Roberto Faedda

Received: 13 July 2023
Revised: 27 July 2023
Accepted: 28 July 2023
Published: 31 July 2023

1. Introduction

Zanthoxylum armatum, a small-sized tree or shrub, is predominantly found in China, Japan, Korea, India, and Pakistan. In China, it is primarily distributed in the southwestern region (21.37° N, 85.121° E) [1]. This species holds great significance in afforestation, rural industrial restructuring, and improving farmers' livelihoods, owing to its capabilities in soil and water conservation [2]. Unfortunately, root rot disease poses a significant threat to *Z. armatum* production, resulting in substantial economic losses in the agricultural and forestry sectors worldwide [3]. Root rot disease of *Zanthoxylum* spp. primarily affects the root system, leading to discoloration and decay of the affected roots. Infected roots emit a foul smell, and the root epidermis easily detaches from the woody tissues. In severe cases, the woody tissues become blackened, spreading along the main root towards the root-stem junction. Above-ground parts of the affected plants show symptoms such as reduced leaf size, chlorosis (yellowing), stunted fruit development, and incomplete branch growth. Ultimately, this condition results in wilting and the eventual death of the plants. Conventional chemical pesticides have proven ineffective in controlling soil-borne

pathogens, particularly due to their soil-based spread and the development of resistance [4]. As a result, there is a growing demand for the development of biological control methods in soil-borne disease management [5,6].

The rhizosphere soil of plants is often referred to as the "second genome of soil" due to its abundance of microorganisms, including fungi, bacteria, nematodes, viruses, and arthropods [7].

Beneficial microorganisms in the rhizosphere play a crucial role in promoting nutrient absorption, safeguarding plants from pathogens, and improving plant resilience to stress. Additionally, these microorganisms contribute to the breakdown of organic substances in the soil, fostering soil fertility and structure [8]. Recent studies focusing on rhizosphere microbial communities have highlighted their significant involvement in plant disease control [9,10], nutrient uptake efficiency, and plant tolerance to abiotic stresses. However, the rhizosphere represents a competitive environment where soil-borne pathogens and rhizosphere microbial communities compete for limited resources and production space, leading to microbial colonization. Soil-borne pathogens can impact the composition and structure of rhizosphere microbial communities. In contrast, soil microbial diversity, composition, and functionality are crucial factors in maintaining long-term ecosystem balance and controlling outbreaks of soil-borne plant diseases [11–13]. Conversely, studies have shown that plants, when invaded by soil-borne pathogens, can shape beneficial microbial communities in the rhizosphere soil by recruiting beneficial microorganisms and enhancing microbial activity to suppress disease occurrence [14–17]. For instance, dominant populations such as *Burkholderia*, *Bacillus*, and *Streptomyces* genera have been found in the healthy soil of *Panax notoginseng* [11], and *Pseudomonas aeruginosa* BA5, obtained from the plant rhizosphere, has demonstrated effective inhibition of mycelial growth of pathogens, with an inhibition rate of 58.33% against the specialized cucumber pathogen *Fusarium oxysporum* [18]. Consequently, it was proposed that the adjustment of the composition and structure of the plant's rhizosphere microbial community can enhance its resistance to pathogens [19–21].

However, the composition and structure of microorganisms are significantly impacted by the presence of plant diseases [22–24]. It is not yet known, though, whether variations in the composition of the community of microorganisms under various health circumstances affect how well plants defend themselves from soil-borne ailments. The rhizosphere of healthy plants contains a larger abundance of good microbes like *Bacillus* than the rhizosphere of diseased plants, according to studies, which show substantial variations in the beneficial microorganisms between the two [15]. *Bacillus* has emerged as a key source of biocontrol products for agricultural management. Moreover, *Bacillus* strains have demonstrated the ability to control plant diseases and promote plant growth. For instance, antagonistic strains capable of inhibiting bacterial wilt disease have been isolated from the rhizosphere soil of infected tomato plants. Research has shown that most biocontrol agents are derived from the rhizosphere soil of healthy plants, and many of these agents have been successfully tested for their disease suppression effects under greenhouse and field conditions.

In this study, we hypothesized that infection by soil-borne pathogens might result in differences in the composition of rhizosphere soil microbial communities between healthy plants and plants infected by root rot disease. These differences could offer valuable insights for screening potential biocontrol strains to defend against soil-borne pathogens. To test this hypothesis, we collected samples of infected root tissues and rhizosphere soil from both infected and healthy *Z. armatum* plants. We isolated and identified the pathogenic fungi from the infected *Z. armatum* root tissues and assessed the physicochemical properties of the infected and healthy plant rhizosphere soils. High-throughput sequencing technology was utilized to gain a comprehensive understanding of the microbial taxa and their relative abundance in the rhizosphere soil of healthy and infected *Z. armatum* plants. Furthermore, we used a culture-based approach to isolate and screen biocontrol bacteria from the rhizosphere soil, followed by testing the strains for their disease-control and

growth-promoting effects. By understanding the impact of root rot disease on rhizosphere microbiota, we aim to gain better insight into the mechanisms of plant disease occurrence and develop appropriate measures for disease control and treatment.

2. Materials and Methods

2.1. Experimental Design

Siwei Village, Taihe Town, Meishan City, Sichuan Province, China (30°04′33″ N; 103°50′54″ E) is where the sample location is situated. This region had an average annual temperature of 17.9 degrees and 855.5 mm in typical annual precipitation in 2021. It is one of China's main centers for the production of Sichuan peppers. The most significant variety among these peppers is *Z. armatum*, and August is the season when it is most likely to contract the illness known as root rot. Twenty sampling locations were established in two 30 m × 30 m *Z. armatum* plant growth areas. Among the sampling locations, ten were found to be free from root rot (Figure 1a,c), while ten others exhibited signs of root rot (Figure 1b,d). The five-point sampling method was employed to collect samples in each plot, with a distance of 500 m between each sampling site. A total of 20 samples were collected, including 10 healthy samples (labeled as HR1-10, HRS) and 10 samples affected by root rot (labeled as DR1-10, DRS). Prior to sample collection, the ground was cleared of dead branches, fallen leaves, and debris. Samples were then collected within a circular area of 0.5 m in diameter, centered around the main stem of the plant. A gentle brushing was performed to remove 2 mm thick soil adhering to the roots, which served as rhizosphere soil samples. The root depth ranged from 0 to 20 cm. The collected samples are placed in 50 mL centrifuge tubes, numbered, sealed, and brought back to the laboratory for storage at −20 °C. The root tissues were stored in a refrigerator at −4 °C.

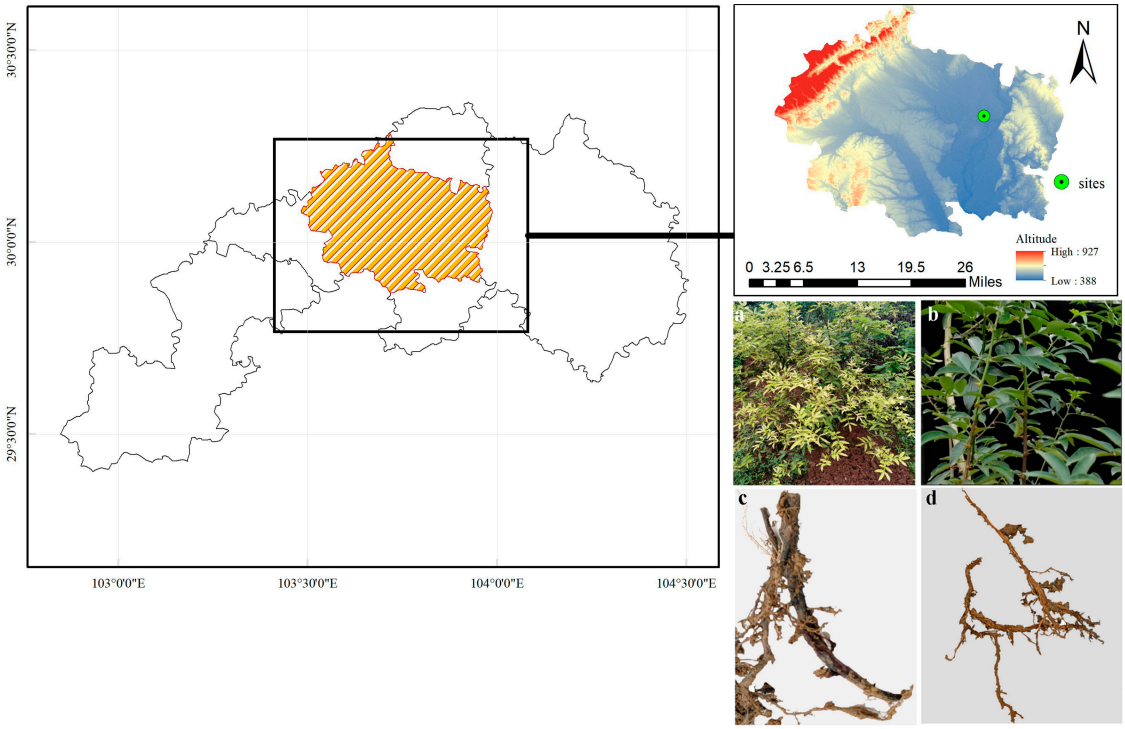

Figure 1. Sampling locations of healthy and diseased *Zanthoxylum armatum* and comparative images of healthy and diseased *Z. armatum*. (**a**,**c**) *Z. armatum* infected with root rot disease; (**b**,**d**) Healthy *Z. armatum*.

2.2. Comparing the Physicochemical Characteristics of Diseased and Healthy Plants' Rhizosphere Soil

Soil pH value was determined by the electrode method. The potassium dichromate oxidation spectrophotometric method was employed to determine soil organic matter (SOM) [25]. The Kjeldahl method was used to measure the concentration of total nitrogen (TN) in the soil [26]. The molybdenum antimony blue colorimetric method was used to detect the concentration of total phosphorus (TP) in the soil [27]. The ammonium acetate method was used to measure the concentration of total potassium (TK) in the soil [28].

2.3. Isolating and Characterizing the Pathogen Causing Root Rot Disease in Z. armatum

Pathogen Isolation and Purification: Following Fang's plant pathology research method [29], ten bamboo leaf pepper root systems displaying symptoms of root rot were collected for the isolation of the fungal pathogens, with slight modifications (Supplementary Materials).

Pathogenicity Test: To confirm the pathogenicity of the isolated fungal strains, a modified version of the bare-root inoculation test was conducted [30]. Twenty healthy *Z. armatum* plants (1 year old) were carefully washed with tap water to clean their root systems, which were then surface sterilized. The pathogenic isolate HJGFB-1, grown on PDA for 7 days, was used. The spore suspension was adjusted to 1×10^7 spores/mL. Sterile filter paper strips (approximately 1 cm wide × 8 cm long) were immersed in the spore suspension for 30 s. Meanwhile, control paper strips were soaked in sterile water for 30 s. The treated paper strips were placed at the top and middle parts of the roots (with 4 replicates for each treatment). The middle part of the root was incised with a sterile surgical blade (approximately 1 cm long and 1 mm deep). Each inoculated root was then wrapped with four layers of sterile, moist gauze and placed in a folded plastic bag. The bags were incubated at 22 ± 1 °C in darkness for 3 weeks. Subsequently, the pathogen was recovered from symptomatic root portions and identified through ITS sequence analysis.

Pathogen Identification: Fungal genomic DNA was extracted from the pathogenic isolates using the Fungi DNA Extraction Kit (TIANDZ, Beijing, China). PCR was performed to amplify the internal transcribed spacer (ITS), DNA-dependent RNA polymerase II subunit (RPB2), β-tubulin (TUB), and translation elongation factor 1-α (TEF1) genes, following the protocol by O'Donnell (1996) [31]. After gel electrophoresis of the PCR products, the amplified PCR products of the antagonistic strains were sent to a specific company for sequencing. The obtained sequences were subjected to BLAST analysis in NCBI GenBank (http://blast.ncbi.nlm.nih.gov/Blast.cgi, accessed on 10 December 2020) to download highly similar reference gene sequences. The MEGA software version 5.0 was used to manually align and remove redundant sequences as required, followed by the construction of a phylogenetic tree containing multiple genes using PhyloSuite (jushengwu.com, accessed on 25 December 2020). The phylogenetic status of the antagonistic bacteria was determined based on the analysis of the gene phylogeny. The nucleotide sequences were deposited in the GenBank database and assigned accession numbers MW350047, MW350046, MW350047, and MW446809, respectively.

2.4. Characterization of Rhizosphere Soil Microbial Microbiome

Microbial DNA was extracted from each sample using the standard protocol of the PowerSoil DNA Isolation Kit (MO BIO Laboratories, Inc., Carlsbad, CA, USA) [15]. The quality and quantity of DNA were evaluated using the 260 nm/280 nm and 260 nm/230 nm ratios. The V3–V4 region of the bacterial 16S rRNA gene was amplified using the forward primer 338F (5′-ACTCCTACGGGAGGCAGCA-3′) and the reverse primer 806R (5′-GGACTACHVGGGTWTCTAAT-3′) [32]. The ITS region of fungal DNA was amplified using the forward primer ITS1 (5′-CTTGGTCATTTAGAGGAAGTAA-3′) and the reverse primer ITS2 (5′-GCTGCGTTCTTCATCGATGC-3′) [33]. The PCR reactions were performed using the Phusion® High-Fidelity PCR Master Mix with GC Buffer from New England Biolabs [34,35]. The PCR amplification was carried out with efficient and high-fidelity

enzymes to ensure amplification efficiency and accuracy. The resulting PCR products were checked using 2% agarose gel electrophoresis (at a voltage of 120 V for 30 min) and then sent to Novogene Biotech Co., Ltd. (Beijing, China) for paired-end sequencing (2 × 250) on the Illumina HiSeq 2500 platform.

2.5. Bioinformatics Analysis

Microbial community analysis was performed using the QIIME (Quantitative Insights Into Microbial Ecology) version 1.7.0 [36]. A total of 142,378 high-quality bacterial sequences and 2,021,972 high-quality fungal sequences, with average lengths of 1447 bp and 241 bp, respectively, were recovered after quality filtering, denoising, merging, and chimeric filtering. Sequences relevant to chloroplasts and mitochondria were eliminated since bacterial 16S rDNA primers can also target those organelles' DNA. Additionally, OTUs were grouped using UPARSE (version 7.1) with a 97% similarity criterion. The UNITE database (version 18.11) and USEARCH database (version 8.0) consensus taxonomy classifier against the SILVA 16S rRNA database (version 1.3.2) were used to classify representative sequences of each fungal and bacterial OUT [37,38]. The acquired sequences of the root zone bacteria and the rhizosphere soil fungus were then uploaded to the NCBI Sequence Read Archive (SRA) with the accession codes PRJNA858954 and PRJNA863757, respectively.

2.6. Isolation of Cultivable Bacterial and Fungal Strains from Rhizosphere Soil

Considering the notable disparity in the relative abundance of *Fusarium* between the rhizosphere soil of healthy and diseased plants, we extracted potential antagonistic microorganisms from the rhizosphere soil of healthy *Z. armatum* plants. The primary process involved the following steps: We transferred 10 g of rhizosphere soil into a 250 mL conical flask, supplemented with 90 mL of sterile water. The soil sample solution was further diluted to 10^{-1}, 10^{-2}, 10^{-3}, 10^{-4}, 10^{-5}, 10^{-6}, and 10^{-7} using sterile water. Subsequently, 100 µL of the solution from the 10^{-4}, 10^{-5}, 10^{-6}, and 10^{-7} dilutions was evenly spread on nutrient agar (NA) plates for bacteria (n = 3 plates) and potato dextrose Agar (PDA) plates for fungi (n = 3 plates). The NA plates were incubated at 37 °C in a bacterial incubator for 24 h, while the PDA plates were incubated at 25 °C in a constant temperature incubator for 5 days. For purification, single colonies with observable morphological differences were chosen and subcultured on NA or PDA medium. Separately inoculated on NA and PDA medium, the purified bacterial and fungal strains were then placed in storage at 4 °C for later use [39].

2.7. Screening and Determination of Antagonistic Effects of Antagonistic Bacteria

Modifying the research methodology based on the study conducted by Lin et al., we employed the plate confrontation method to investigate the antagonistic effects of several microbial strains on the growth and development of the pathogenic fungus *F. solani*. Single colonies exhibiting antagonistic activity were selected and inoculated into 50 mL/250 mL of LB broth, followed by continuous shaking (180 rpm) for 24 h at 28 °C. The screening of antagonistic bacteria involved placing the pathogenic fungus (diameter d = 8 mm) on one side of a PDA plate and making a sterile hole with a diameter of 6 mm, 3 cm away from the fungus on the other side of the plate. Then, 100 µL of bacterial culture medium was injected into the sterile hole. The control plate contained only the pathogenic fungus and sterile water, with sterile water being injected into the sterile hole on the PDA plate. The pathogenic fungus (diameter d = 8 mm) was put on one side of a PDA plate for the purpose of screening antagonistic fungi, and a sterile 8 mm hole was constructed 3 cm distant from the fungus. Then, 2 µL of bacterial fermentation broth was dropped into the sterile hole. In accordance with the method outlined by Ritpitakphong et al. [40] the sizes of the lesions caused by the pathogenic fungus were assessed following a 7-day cultivation period at 28 °C. Each antagonistic strain was subjected to three repetitions to ensure accuracy and reliability of the measurements.

In potted plants, the antagonistic bacteria's capacity to prevent *Z. armatum* plant root rot was assessed. Each planting bag included 500 g of the substrate (soil:vermiculite:peat = 2:1:2, *V*/*V*) before being sterilized under high pressure. Each bag was then sealed for 7 days of cultivation after being injected with 10 mL of hostile bacterial fermentation broth. With five replicates for each treatment, sterile water injected into the soil medium at an identical volume served as the control. A sterile syringe needle was used to puncture the roots of healthy one-year-old *Z. armatum* plants after they had been cleaned with sterile water for 30 min, dried, and punctured. The wounded plants were transplanted into the aforementioned substrate and grown continuously for 7 days before being inoculated with a 10 mL suspension of *F. solani* spores (1×10^7 spores/mL). All plants were cultured in a greenhouse with a photoperiod of 16 h light and 8 h dark, a humidity of 60%, and a temperature of 25 °C. The occurrence rate of root rot and the mortality rate of plants were observed and assessed every 5 days for up to 20 days, and the disease index [41] of the plants was calculated.

2.8. Identification of Purified Microbial Strains with Potential Antagonistic Activity

The DNA of antagonistic bacterial strains was extracted using the Tiangen Bacterial Genome Kit. The extracted genomic DNA of the tested bacterial strains was used as a template for amplifying the 16S rDNA, gyrA, and gyrB genes of the strains using universal bacterial primers [42,43]. After gel electrophoresis to confirm the PCR products, the PCR products of the antagonistic bacterial strains were sent to a sequencing company for sequencing. The obtained sequences were subjected to BLAST analysis in the NCBI GenBank (http://blast.ncbi.nlm.nih.gov/Blast.cgi, accessed on 29 August 2022), and highly similar and relevant gene sequences were downloaded. Based on the BLAST results, the MEGA software (version 5.0) was used to manually align and remove unnecessary sequences as needed. The IQTREE software was then used to construct a phylogenetic tree using multiple genes. The phylogenetic analysis of the gene evolution was performed to determine the phylogenetic status of the antagonistic bacteria. The nucleotide sequences were stored in the GenBank database, and the accession numbers were obtained (Table 1). As no antagonistic fungal strains were obtained in this experiment, no identification of antifungal strains was performed.

Table 1. GenBank numbers for identification of antagonistic strains.

Sample	16S	gyrA	gyrB
T1	OP317514	OQ659395	OQ659398
T2	OP324656	OQ659396	OQ659399
T3	OP317360	OQ659397	OQ659400

Note: T1 is *B. subtilis*, T2 is *B. amyloliquefaciens*, T3 is *B. siamensis*.

2.9. Statistical Analysis

The R environment (version: V3.6.0, http://www.r-project.org/, accessed on 1 May 2022) was used to conduct all statistical analyses. The "vegan" package in R was used to investigate alpha diversity indices such as the Shannon, Simpson, and Chao1 indices [42]. ANOVA was used to investigate how distinct samples' alpha diversity indices varied from one another. The Kruskal–Wallis test was used to assess differences between the abundance and enrichment levels of bacterial and fungal taxa, and the "ggplot2" package in R was used for display [39]. A generalized linear model (GLM) technique was employed in conjunction with the EdgeR program to identify operational taxonomic units (OTUs) that have differences in abundance [44].

Using principal coordinate analysis (PCoA) based on Bray–Curtis dissimilarity, the beta diversity of rhizosphere soil microbial communities was assessed. The beta diversity of soil microbial communities as determined by PCoA was used to analyze the size and importance of the impacts of season and illness [32]. To evaluate the association between disease severity markers (% of *Fusarium* lesion area and relative abundance) and the

compositional distribution of microbial communities, redundancy analysis (RDA) was used. Using FUNGuild and PICRUSt2, functional prediction of bacterial and fungal OTUs was carried out [38,45,46].

3. Results

3.1. Isolation and Identification of the Pathogen Causing Root Rot in Z. armatum

Eight strains were obtained from diseased roots of *Z. armatum*, and pathogenicity testing identified a highly pathogenic strain, HJGFB-1. The morphological characteristics of this strain on PDA medium included smooth, branched hyphae with septa, transparent appearance, and light brown color. The conidia produced on conidiophores were simple to branches. The conidia consisted of one or two cells and were elliptical or kidney-shaped, varying in size from 3.4 to 5.6 × 7.5 to 12.3 µm (n = 50 conidia). The macroconidia were crescent-shaped with 3–4 septa and a characteristic foot-shaped basal cell, ranging in size from 3.3 to 7.9 × 21.2 to 47.1 µm (n = 50 conidia). The chlamydospores produced intercalarily in the hyphae had thick walls and were produced in chains, measuring 8.5 to 11 × 7.6 to 9 µm (Figure 2).

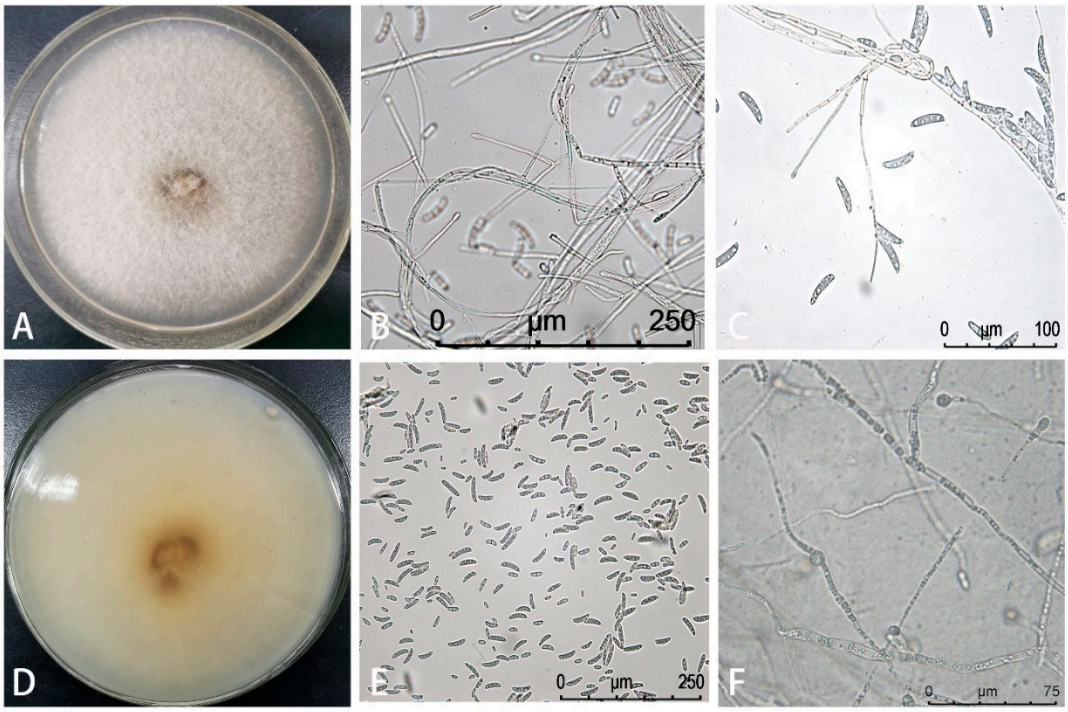

Figure 2. Pathogen morphology. (**A**,**D**): Top and bottom views of *Fusarium solani* on PDA incubate at 25 °C in the dark with light/dark, 14/10 h for 7 days; (**B**): the structure that produces conidia; (**C**): hyphae and macroconidia; (**E**): hyphae; (**F**): chlamydospores.

DNA sequencing and BLAST analysis of the *ITS*, *RPB2*, *TUB*, and *TEF1* gene sequences of this strain showed 99% identity with *F. solani* sequences (GenBank accession numbers KU321553, MK968890, MH888086, and MN652888). A phylogenetic tree was inferred from a combined dataset (*ITS*, *TEF1*, *TUB*, and *PRB2* genes) of *Fusarium* complex members analyzed in this study. The phylogenetic tree demonstrated 100% branch support, indicating a match between the isolated strain and *F. solani* (Figure S1). Based on the morphological features and multi-gene phylogenetic analysis, the isolate was identified as *F. solani*. The root systems of the inoculated plants exhibited brown discoloration and softening of lateral roots, while the roots of the control plants remained healthy with well-developed lateral root systems. The experiment was repeated three times.

In summary, *F. solani* was successfully re-isolated from diseased tissues, and its identity was confirmed based on morphological and sequencing analysis, thus fulfilling Koch's postulates.

3.2. Impact of Fusarium Abundance on the Overall Taxonomic Distribution of Rhizosphere Soil Microbial Communities

The relative abundance of *Fusarium* in the rhizosphere soil of diseased plants was significantly higher compared to that in the rhizosphere soil of healthy plants (Figure 3). Therefore, we analyzed the overall taxonomic classification and distribution of rhizosphere soil microbial communities in response to the increased abundance of *Fusarium*. The results showed that a total of 3689 bacterial operational taxonomic units (OUTs) and 1771 fungal OUTs were obtained from the rhizosphere microbiota of healthy and diseased *Z. armatum* plants, with lower fungal diversity compared to bacterial diversity. The fungal community OTUs were associated with 13 phyla, 32 classes, 65 orders, 127 families, 226 genera, and 293 species, while the bacterial community OTUs were associated with 36 phyla, 48 classes, 96 orders, 169 families. Venn diagrams showed that there were 666 shared fungal ASVs and 1347 shared bacterial OUTs between healthy and diseased *Z. armatum* plants. Furthermore, healthy *Z. armatum* plants harbored 1086 fungal OTUs and 2213 bacterial OTUs, while diseased *Z. armatum* plants had 1351 fungal OTUs and 2823 bacterial OTUs. Additionally, principal component analysis (PCA) of the physicochemical properties of the rhizosphere soil in healthy and diseased *Z. armatum* plants revealed significant differences in the soil characteristics between healthy and diseased plants in response to the increased abundance of *Fusarium*.

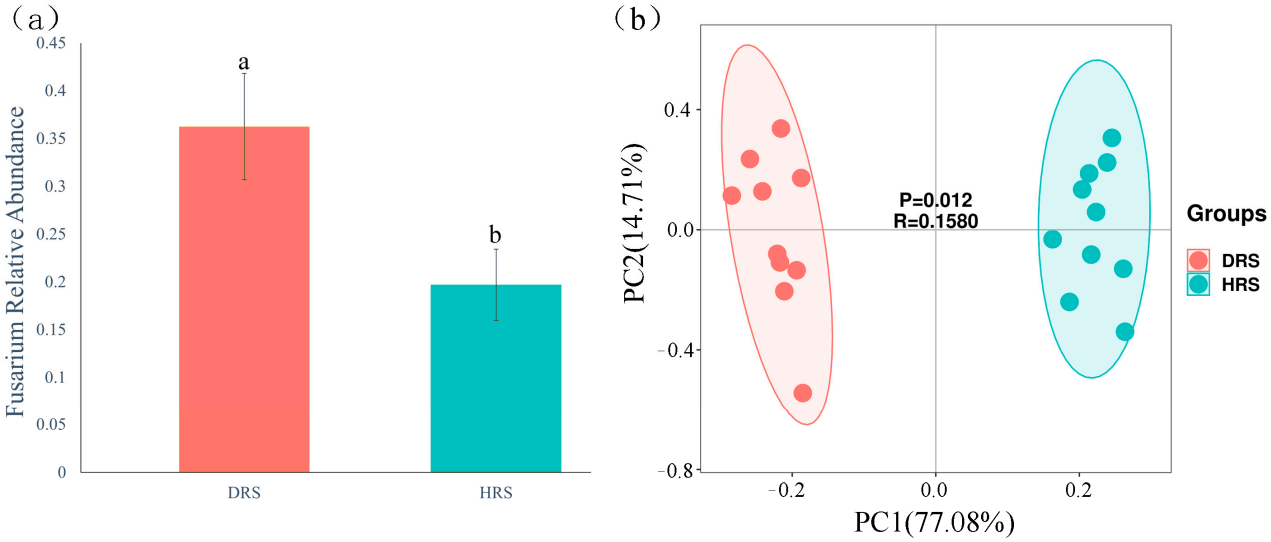

Figure 3. Analysis of the rhizosphere soil characteristics in healthy and diseased *Z. armatum*. (**a**) Comparative analysis of the relative abundance of Fusarium in the rhizosphere soil of healthy and diseased *Z. armatum*. Different letters indicate significant differences among treatments at $p < 0.05$ according to one way ANOVA. (**b**) Principal component analysis (PCA) of the rhizosphere soil of healthy and diseased *Z. armatum* samples. Ellipses represent the 95% confidence intervals. HRS—healthy plant rhizosphere soil, DRS—diseased plant rhizosphere soil.

3.3. Study on the Diversity of Rhizosphere Soil Microbial Communities

The α-diversity of fungal and bacterial communities in the rhizosphere soil of healthy and diseased *Z. armatum* plants was assessed using Shannon, Chao1, Simpson, and good-coverage indices. The fungal Shannon, Chao1, and Simpson indices showed significant differences in diversity between diseased and healthy rhizosphere soil (Wilcoxon test, $p < 0.05$). The results indicated that the presence of diseased plants increased the diversity of rhizosphere soil microbial communities (Figure 4a,b). Regarding the α-diversity of

bacterial communities, there was also a significant difference in microbial diversity between the rhizosphere soil of diseased and healthy plants (Wilcoxon test, $p < 0.05$), with the diseased plants exhibiting a 6.41% increase on the Shannon index and a 47.69% increase on the Chao1 index compared to healthy plants (Figure 4e,f).

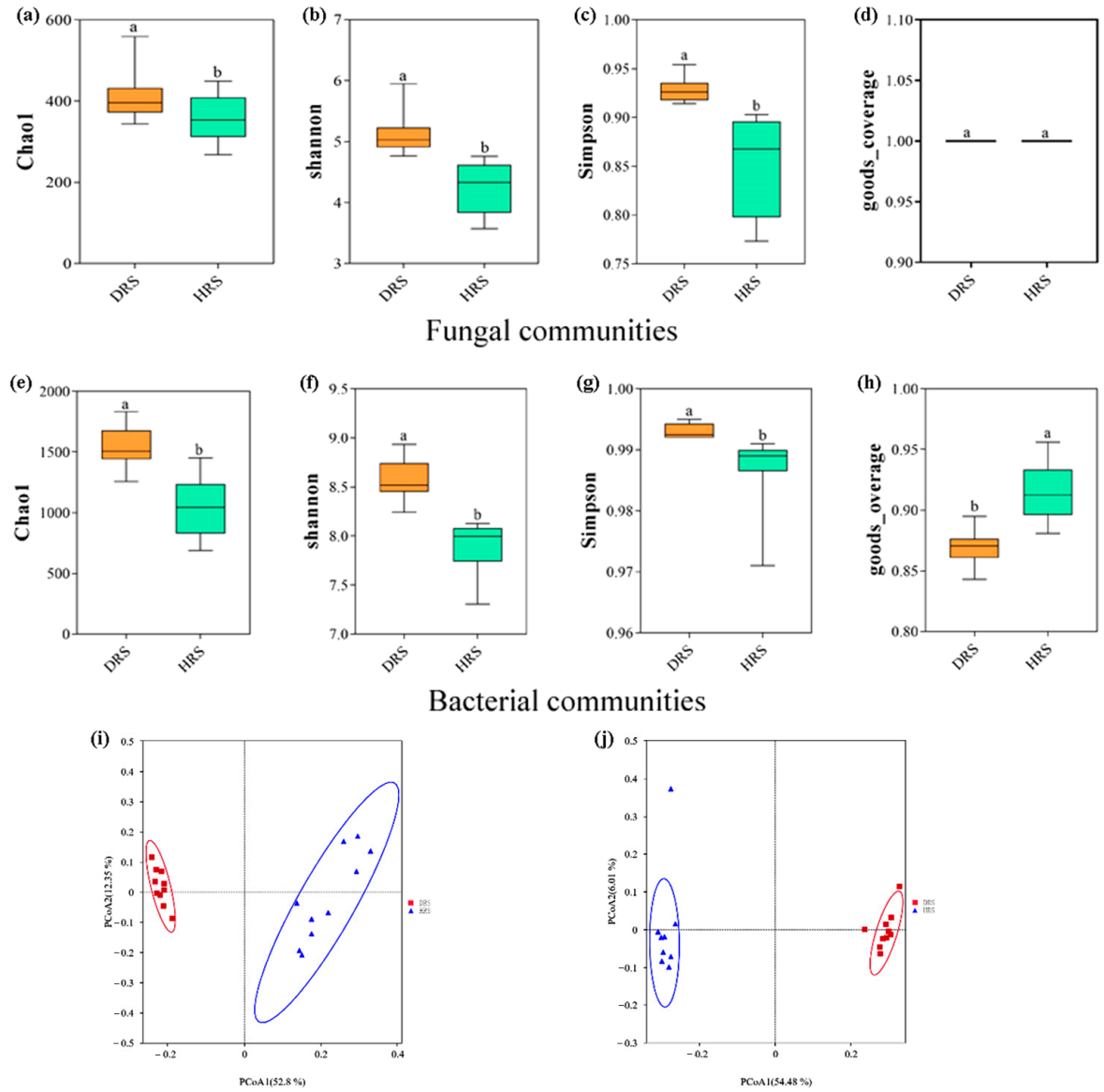

Figure 4. The box plot shows alpha diversity indices of fungal (top) and bacterial (bottom) communities under different treatments. Fungal diversity indices: Chao 1, Shannon, Simpson, and good coverage (**a**–**d**). Bacterial diversity indices: Chao 1, Shannon, Simpson, and good coverage (**e**–**h**). Treatments: diseased rhizosphere soil (DRS), healthy rhizosphere soil (HRS). Lowercase letters on each box plot indicate significant differences among treatments (Wilcoxon test, $p < 0.05$). Principal coordinate analysis (PCoA) based on the Bray–Curtis distance matrix demonstrates the separation between soil bacterial and fungal communities under different treatments. PCoA for bacterial (**i**) and fungal (**j**) communities.

Principal coordinate analysis (PCoA) was performed to assess the β-diversity of soil microbial communities, and distinct separation was observed between fungal and bacterial communities derived from the rhizosphere soil of healthy and diseased plants. According to the PCoA results, the first two axes explained 54.48% and 6.01% of the total variance in the bacterial community and 52.82% and 12.35% of the total variation in the

fungal community, respectively (Figure 4i,j). Non-metric multidimensional scaling (NMDS) analysis of pairwise distances variance between bacteria (R^2 = 0.5419, $p < 0.001$) and fungi (R^2 = 0.5083, $p < 0.001$) showed substantial differences in the composition of rhizosphere microbial communities among different health conditions. This indicates that root rot significantly influences the species and composition of bacterial and fungal populations.

3.4. Analysis of Rhizosphere Soil Microbial Community Abundance in Z. armatum

The relative abundance and composition of fungal and bacterial communities in the rhizosphere soil of healthy and diseased *Z. armatum* plants were differentiated based on their most common categories. The richest fungal categories in the rhizosphere soil fungal community were Sordariomycetes (45%), Agaricomycetes (18%), and Eurotiomycetes (12%). Among them, the relative abundance of the fungal class in the rhizosphere soil of diseased plants was 6.88% higher than that in the rhizosphere soil of healthy plants. On the other hand, the most abundant bacterial categories in both healthy and diseased *Z. armatum* rhizosphere soil were Gammaproteobacteria (24%), Acidobacteriia (22%), Alphaproteobacteria (14%), Bacteroidia (9%), and Deltaproteobacteria (6%) (Figure 5a,b).

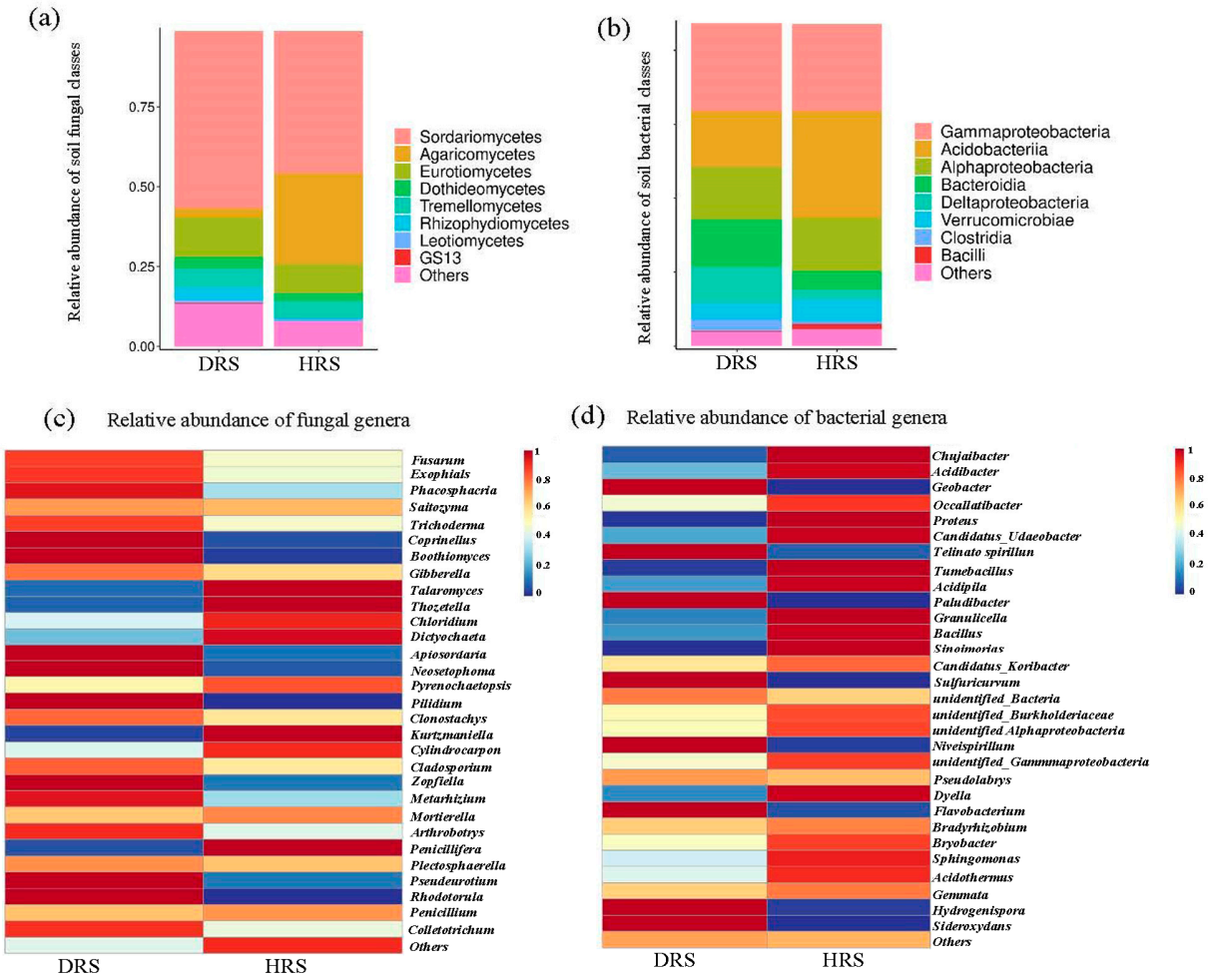

Figure 5. Heatmap of fungal and bacterial communities in the rhizosphere soil of healthy and diseased *Z. armatum* plants. (**a**) Fungal community; (**b**) Bacterial community. Fungal and bacterial taxa that could not be identified at the class level were grouped as "others." (**c**) Heatmap clustering of the top 30 abundant fungal genera. (**d**) Heatmap clustering of the top 30 abundant bacterial genera. Cluster analysis was performed using the Bray–Curtis method, and genera and samples were clustered using the average method. DRS: Diseased plants rhizosphere soil; HRS: healthy plants rhizosphere soil.

A clustering heatmap was used to examine the differences in the top 30 abundant fungal and bacterial genera in the rhizosphere soil of healthy and diseased *Z. armatum* plants (Figure 5c,d). In the rhizosphere soil of healthy *Z. armatum* plants, the following fungal genera were more abundant: *Pyrenochaetopsis*, *Chloridium*, *Cylindrocarpon*, *Dictyochaeta*, *Talaromyces*, *Thozetella*, *Kurtzmaniella*, *Penicllifera*. The rhizosphere soil of diseased *Z. armatum* plants had higher abundance of the fungal genera *Trichoderma*, *Fusarium*, *Exophiala*, *Colletotrichum*, *Arthrobotrys*, *Metarhizium*, *Phaeosphaeria*, *Pseudeurotium*, *Zopfiella*, *Apiosordaria*, *Neosetophoma*, *Coprinellus*, *Rhodotorula*, *Pilidium*, and *Boothiomyces*.

The clustering heatmap analysis of bacterial genera in the rhizosphere soil of *Z. armatum* plants showed that healthy rhizosphere soil had a higher relative abundance of genera such as *Chujaibacter*, *Sinomonas*, *Proteus*, *Tumebacillus*, *Acidibacter*, *Granulicella*, *Dyella*, *Candidatus_Udaeobacter*, *Acidipila*, and *Bacillus*. On the other hand, the rhizosphere soil of diseased plants had a higher relative abundance of genera such as *Telmatospirillum*, *Flavobacterium*, *Niveispirillum*, *Hydrogenispora*, *Geobacter*, *Sideroxydans*, *Paludibacter*, and *Sulfuricurvum*.

3.5. Relationship between Soil Physicochemical Properties and Microbial Community Composition

The relationship between soil physicochemical properties and microbial community composition was investigated. The main physicochemical characteristics of diseased and healthy rhizospheric soils were determined according to the experimental design. The Mantel test indicated significant variations ($p < 0.05$) in soil physicochemical properties, including pH, SOM, TP, TK, and TN, between different health conditions. RDA was used to test and visualize the associations between soil properties and microbial community composition (Figure 6a,b). The results showed that the first two axes explained more than 90% of the fungal and bacterial community structure, with RDA1 explaining the majority of the variation. Based on the length of the vectors, pH, SOM, TP, TK, and TN were identified as the main factors influencing the differences in fungal and bacterial communities. Furthermore, a Spearman correlation heatmap revealed significant positive correlations between TN, SOM, pH, and fungi such as *Fusarium*, *Pseudeurotium*, *Boothiomyces*, *Trichoderma*, *Exophiala*, *Neosetophoma*, *Apiosordaria*, and *Zopfiella*, while negative correlations were observed with TK and TP. The soil physicochemical properties TK and TP exhibited positive correlations with bacterial genera such as *Acidibacter*, *Dyella*, *Proteus*, *Chujaibacter*, *Occallatibacter*, *Acidipila*, *Granulicella*, *Bacillus*, and *Bryobacter* (Figure 6c,d).

3.6. Functional Prediction of Fungal and Bacterial Taxa

Functional predictions of fungal communities in diseased and healthy plant rhizospheric soils were analyzed using FUNGuild (Figure 7a). The results showed significant differences ($p < 0.05$) in fungal functional profiles between diseased and healthy rhizospheric soils, including animal pathogen, soil saprotroph, animal endosymbiont—undefined saprotroph, dung saprotroph—undefined saprotroph, and dung saprotroph. Additionally, functional predictions of bacterial communities in diseased and healthy rhizospheric soils were performed based on the KEGG database (https://www.kegg.jp/, accessed on 25 August 2022) using PICRUSt2 (Figure 7b). The results revealed 30 secondary functional categories in the bacterial communities, including sorting and degradation, aging, amino acid metabolism, biosynthesis of other secondary metabolites, cancer: overview, cancer: specific types, carbohydrate metabolism, cell growth and death, cell motility, cellular community—eukaryotes, cellular community—prokaryotes, circulatory system, cevelopment and regeneration, digestive system, drug resistance: antimicrobial, drug resistance: antineoplastic, endocrine and metabolic disease, endocrine system, energy metabolism, environmental adaptation, excretory system, folding, glycan biosynthesis and metabolism, immune disease, immune system, infectious disease: bacterial, infectious disease: parasitic, infectious disease: viral, and lipid metabolism. Among these, there were significant differences ($p < 0.05$) in the cellular community—eukaryotes function between bacterial communities in diseased and healthy plant rhizospheric soils.

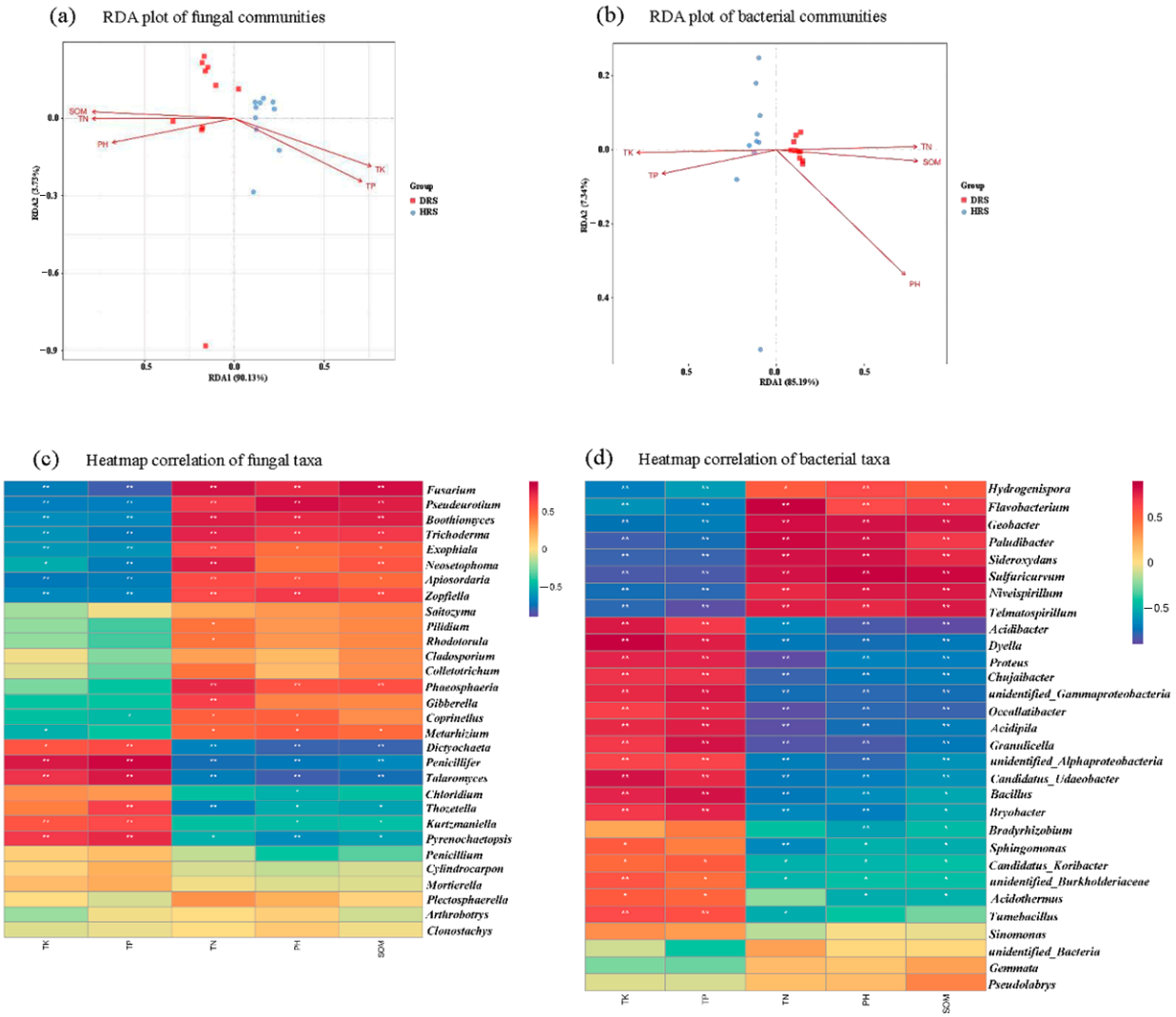

Figure 6. Redundancy analysis (RDA) and Spearman correlation heatmaps were utilized to explore the relationships between the relative abundance of key microbial genera and soil physicochemical properties in the rhizosphere soil of diseased and healthy *Z. armatum* plants. (**a**) RDA plot displaying fungal taxa. (**b**) RDA plot displaying bacterial taxa. (**c**) Spearman correlation heatmap illustrating the relationships among fungal taxa. (**d**) Spearman correlation heatmap illustrating the relationships among bacterial taxa. DRS: Diseased plants rhizosphere soil; HRS: Healthy plants rhizosphere soil. The significance levels of Spearman correlation are denoted as follows: * $p \leq 0.05$; ** $p \leq 0.01$.

3.7. Screening of Antagonistic Bacteria and Determination of Their Antagonistic Effects

A total of 48 bacterial strains were isolated and purified from healthy rhizospheric soil. The antagonistic activity of these strains was screened using the plate confrontation method, and three bacterial strains showed significant inhibitory effects against the pathogenic fungus *F. solani*. Specifically, the lesion size of *F. solani* grown on the culture medium mixed with the bacterial strains (T1, T2, T3) was compared to the lesion size on the control plate. It was observed that T1, T2, and T3 exhibited an average reduction of 52.94%, 46.06%, and 48.23%, respectively (Figure 8a).

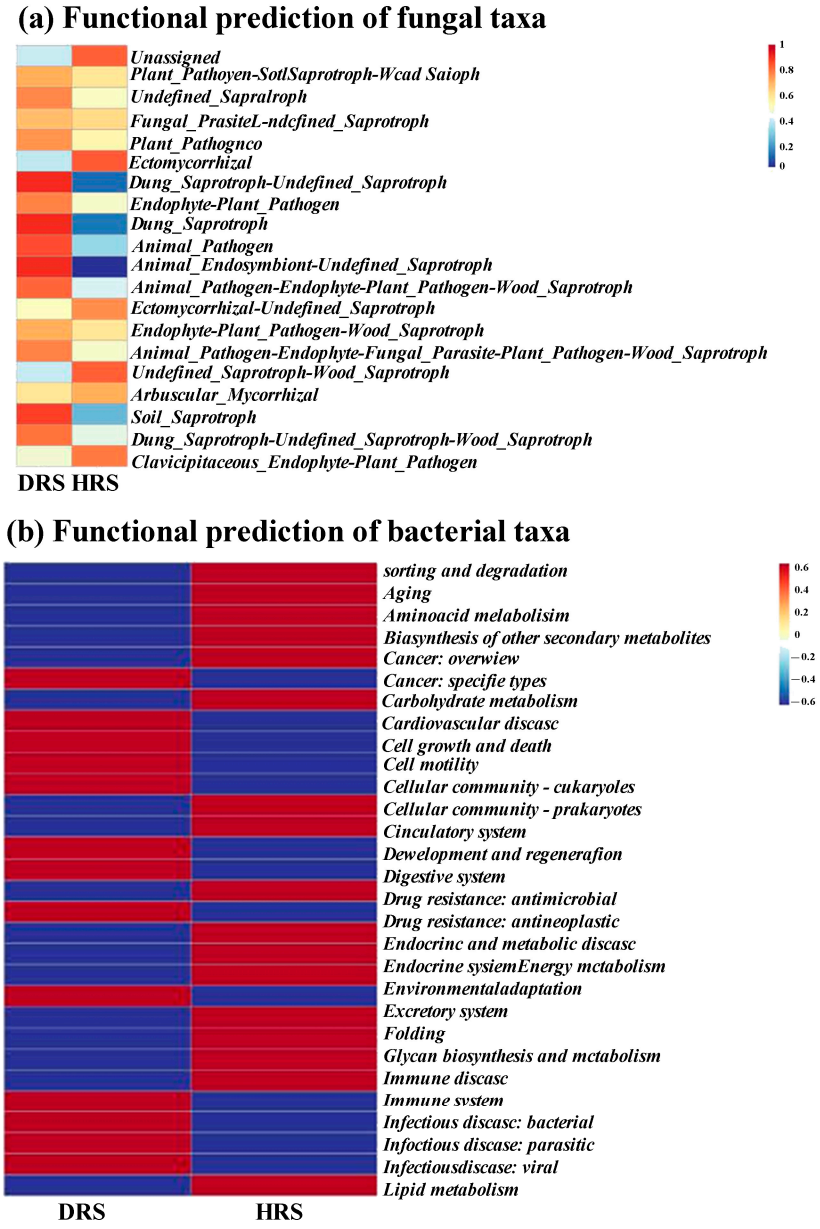

Figure 7. Functional predictions of fungal and bacterial taxa in the rhizosphere soil of healthy and diseased *Z. armatum* plants were performed using FUNGuild and PICRUSt2, respectively. (**a**) Variations in fungal functional group compositions predicted by FUNGuild. (**b**) Variations in bacterial functional group compositions predicted by PICRUSt2. DRS: Diseased plants rhizosphere soil; HRS: Healthy plants rhizosphere soil.

Moreover, the three biocontrol bacterial strains were evaluated on *Z. armatum* plants that were infected with *F. solani*. The outcomes demonstrated a progressive increase in the disease index of the positive control plants, which were solely inoculated with *F. solani* spore suspension. In contrast, the disease index of *Z. armatum* plants treated with spore suspensions of the antagonistic bacterial strains (T1, T2, T3) initially increased but subsequently declined, in comparison to the positive control plants. These findings provide evidence of the potent inhibitory effects exerted by the three antagonistic bacterial strains on the growth and pathogenicity of *F. solani*, both in vivo and within vitro (Figure 8b).

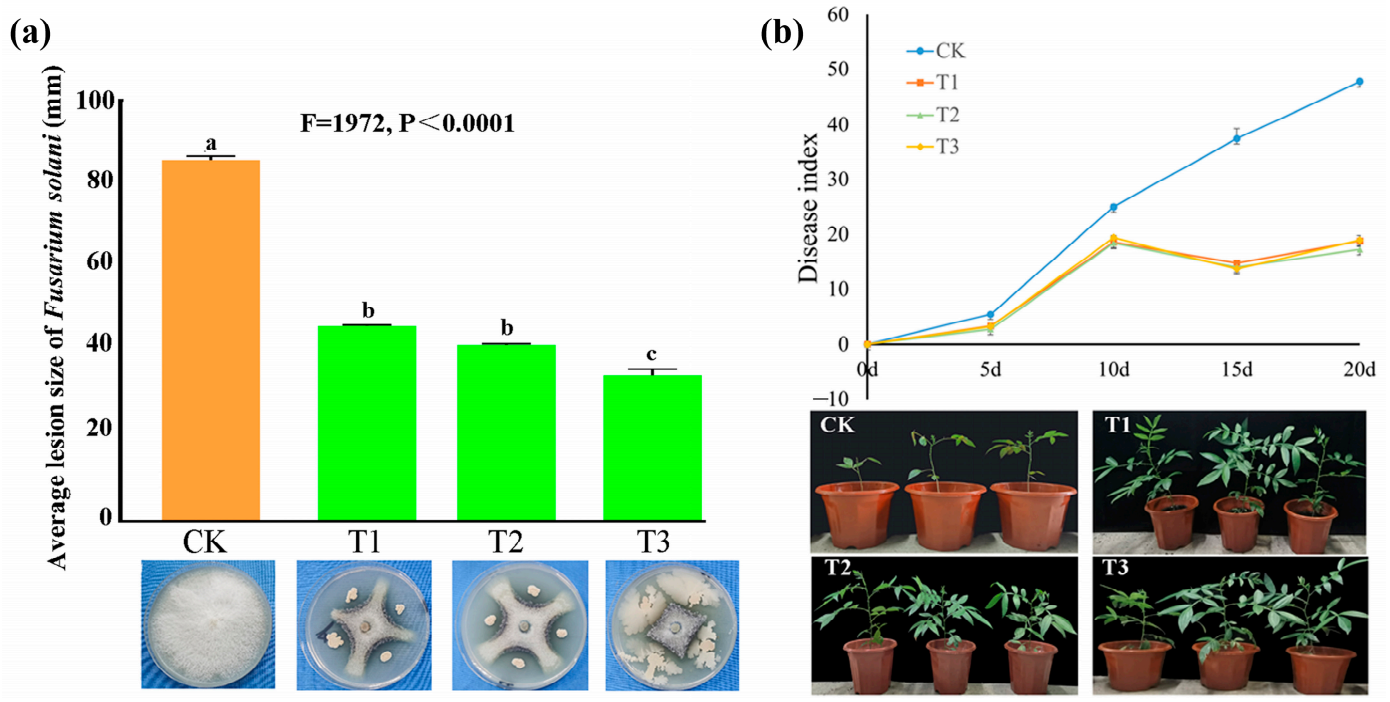

Figure 8. The antagonistic effect of bacterial strains (T1, T2, and T3) isolated from the rhizosphere soil of healthy *Z. armatum* plants on the growth of the pathogenic fungus, *F. solani*. (**a**) Average lesion size caused by *F. solani*. (**b**) Disease index after applying bacterial strains T1, T2, and T3, respectively, to prevent and control *F. solani* infection in *Z. armatum* plants. Each strain was tested on three plates. The values represent means ± SE. Based on one-way ANOVA, different letters indicate significant differences among treatments at $p < 0.05$. CK: *F. solani*, T1: *B. amyloliquefaciens*, T2: *B. subtilis*, T3: *B. siamensis*. Each strain was tested on three plates. The values represent means ± SE.

3.8. Identification of Antagonistic Bacteria

The morphological characteristics of the three antagonistic bacterial strains are shown in Figure 9. Strain T1 has a wrinkled, irregular, white colony surface and exhibits chain-shaped rod cells. Strain T2 appears as a light yellow, opaque colony with a rough surface, protrusions, and irregular edges on LB agar medium. Strain T3 has a flat, smooth, moist, opaque colony surface with a light-yellow color. Gram staining of all three bacterial strains showed positive results.

Based on bacterial molecular biology identification, sequencing of the 16S rRNA, gyrA, and gyrB genes was performed. The obtained sequences were subjected to BLAST nucleotide sequence alignment in the NCBI database. The results confirmed that all three biocontrol strains belong to the genus *Bacillus*. The alignment of 16S rRNA, gyrA, and gyrB sequences showed that T1 exhibited 100% homology with *Bacillus subtilis*, T2 exhibited 99% homology with *Bacillus amyloliquefaciens*, and T3 exhibited 99% homology with *Bacillus siamensis* (Figures 10 and 11).

Maximum likelihood and Bayesian posterior probability analyses were conducted using IQtree v.1.6.8 and MrBayes v.3.2.6 to infer the phylogenetic relationships of T1, T2, and T3 with related taxonomic groups based on concatenated sequences of the 16S rRNA and gyrA genes. The nodes in the phylogenetic tree represent the RAxML bootstrap support values (ML $\geq$ 50) and Bayesian posterior probabilities (PP $\geq$ 90) (ML/PP).

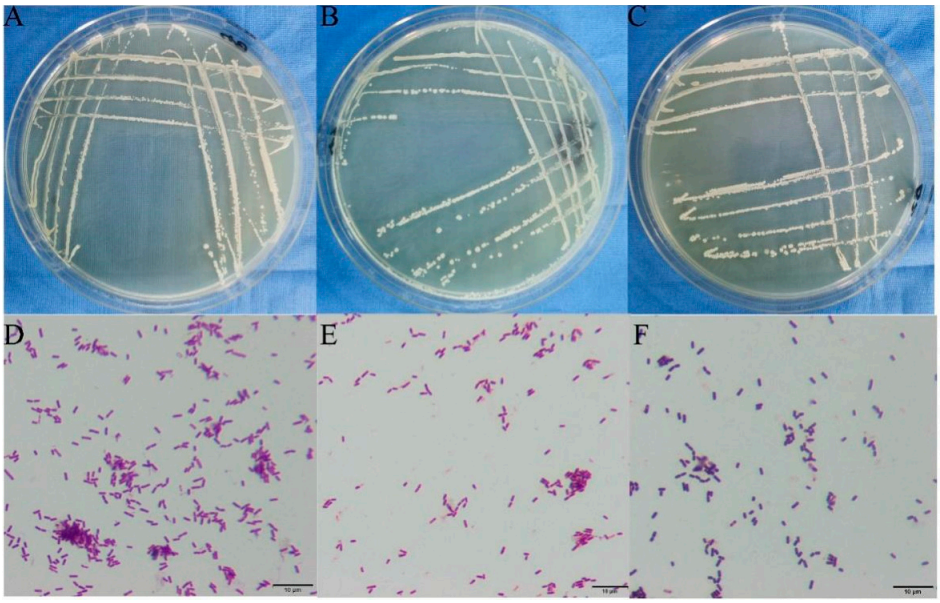

Figure 9. Colony morphology and microscopic morphology observation of biocontrol bacteria; (**A**,**D**): *B. subtilis*, (**B**,**E**): *B. amyloliquefaciens*, (**C**,**F**): *B. siamensis*.

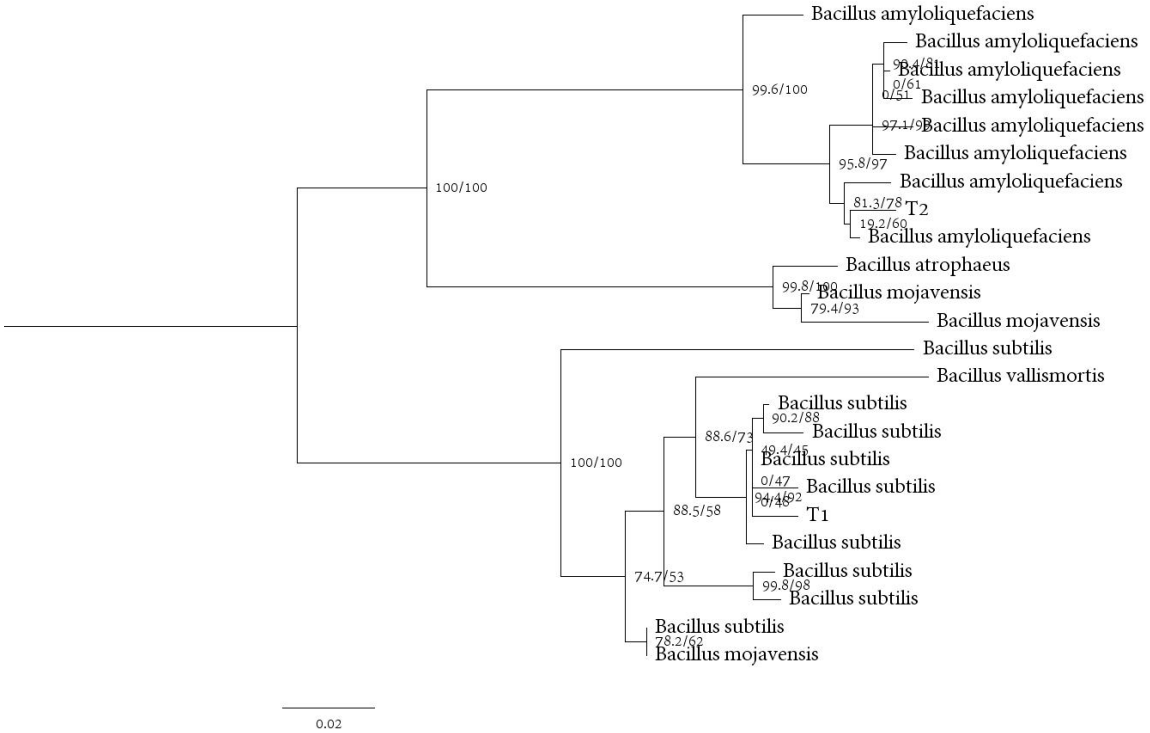

Figure 10. Phylogram generated from Bayesian inference analysis based on combined sequences of 16S and gyrA from 24 recognized *Bacillus* species. Bootstrap support values greater than 0.5 are indicated above/below the nodes. The ex-type (ex-epitype) and voucher stains are in red font. Confirmed that T1 is *Bacillus subtilis* and T2 is *Bacillus amyloliquefaciens*.

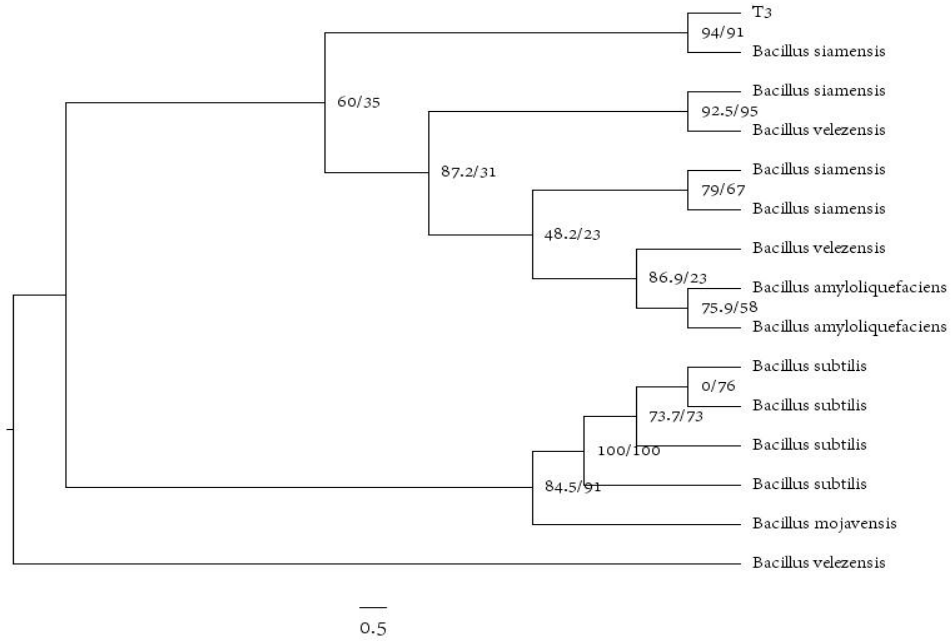

Figure 11. Phylogram generated from Bayesian inference analysis based on combined sequences of 16S and gyrA from 24 recognized *Bacillus* species. Bootstrap support values greater than 0.5 are indicated above/below the nodes. The ex-type (ex-epitype) and voucher stains are in red font. Confirmed that T3 is *B. siamensis*.

4. Discussion

In this study, we isolated and identified the pathogenic fungus causing root rot in the *Z. armatum* plant. Based on morphological characteristics and multi-gene phylogenetic analysis, we confirmed that the pathogen responsible for *Z. armatum* root rot disease is *F. solani* (Figure 1 and Figure S1) [47]. Soil microbial characteristics can to some extent reflect soil quality and health. When soil-borne diseases occur, there are often significant differences in microbial diversity and intergroup dynamics between healthy and diseased plant rhizosphere soils [48]. Higher microbial community diversity indices indicate more complex community structures and greater stability, thus enhancing the ability to cope with environmental changes and pathogen invasion [49,50]. In this study, we found that the infection of *Z. armatum* plant roots with root rot led to an increase in the diversity of fungi and bacteria in the rhizosphere soil. The Chao 1 and Shannon indices of the rhizosphere soil of diseased plants were significantly higher than those of healthy plants. This result is inconsistent with the changes in microbial diversity observed in common soil-borne diseases, but a similar phenomenon has been found in the rhizosphere soil of *Panax notoginseng* infected with root rot [11]. The differential response may be due to changes in the rhizosphere soil ecological conditions of *Z. armatum* plants caused by the occurrence of root rot disease, promoting the growth and reproduction of certain microorganisms and thereby increasing the species diversity of rhizosphere soil microorganisms. In this study, we compared the relative abundance of *Fusarium* in the rhizosphere soil of healthy and diseased *Z. armatum* plants during the peak period of root rot. The results showed that the amount of *Fusarium* was significantly higher in the rhizosphere soil of diseased plants compared to healthy plants. We also found significant differences in soil physicochemical properties between healthy and diseased rhizosphere soils (Figure 6). Soil physicochemical properties can indirectly affect the composition and relative abundance of rhizosphere microorganisms by influencing plant physiology. Our study found that the content of SOM, pH, and TK in the rhizosphere soil of diseased *Z. armatum* plants was higher than that in healthy plants, which may be attributed to the high content of humus in the rhizosphere soil caused by root rot infection. There is increasing evidence that the structure of rhizosphere-associated soil microbial communities differs greatly between healthy and diseased plants,

indicating that plants can recruit beneficial microorganisms in their rhizosphere to suppress soil-borne pathogens.

Therefore, we further analyzed the compositional differences of bacterial and fungal taxa in the rhizosphere of healthy and diseased *Z. armatum* plants and found that the rhizosphere soil of *Z. armatum* plants harbored a rich abundance of ecologically beneficial bacterial genera, with the *Bacillus* sp. being higher in healthy plant rhizosphere microbiota compared to diseased plant rhizosphere microbiota. Currently, *Bacillus*-based biocontrol agents have been widely developed and applied in various fields such as agriculture, forestry, livestock, and fisheries [51]. Previous studies have demonstrated that several species within the genera *Bacillus* possess strong biocontrol capabilities by producing a wide range of antagonistic compounds. Additionally, *Bacillus* spp. can assist plants in acquiring nutrients such as nitrogen and phosphorus, promote plant hormone synthesis, enhance the host plant's nutrient utilization efficiency, and improve its tolerance to biotic and abiotic stresses. *Bacillus*-based biocontrol agents have been applied in the management of *Fusarium* crop diseases and agricultural environmental pollution [52,53]. For example, *B. velezensis* has been used to control root rot disease in *Z. armatum* [54]; *B. amyloliquefaciens* has shown biocontrol activity against *Xanthomonas* sp. and the potential as a biocontrol agent for bacterial diseases in rice [55]. Additionally, research has shown that *Bacillus* spp. has the ability to suppress the growth of *Colletotrichum gloeosporioides* and *F. oxysporum* [5].

We isolated cultivatable bacterial strains from the soil near healthy plants' rhizomes and tested them in vivo and in vitro for their ability to suppress the pathogenic fungus *F. solani*. This further confirms the suppressive impact of rhizosphere microbial communities on soil-borne pathogens. Results showed that three bacterial strains, *B. subtilis*, *B. amyloliquefaciens*, and *B. siamensis*, isolated from soil in the rhizosphere had strong inhibitory effects on *F. solani*. In addition, we found that healthy plants had a greater variety of *Bacillus* spp. in their rhizosphere soil than did sick plants. In conclusion, we have shown that healthy *Z. armatum* plants are able to prevent infection with the soil-borne pathogen *F. solani* by recruiting hostile bacteria in the soil of the rhizosphere.

5. Conclusions

This research revealed that *F. solani* is the main culprit responsible for *Z. armatum* root rot, and that plants infected with *F. solani* demonstrated a high *Fusarium* abundance in their rhizosphere soil. Furthermore, microbial community research revealed that healthy *Z. armatum* plants possess a greater quantity of beneficial microbial groups in the rhizosphere soil, suggesting that these microbes may function as biocontrol agents. The rhizosphere soil of healthy plants was sampled, and three bacterial strains were identified as potential biocontrol agents. Both in vitro and in vivo testing demonstrated their antifungal activity against *F. solani*. This study greatly expands our understanding of the structural and functional differences between rhizosphere soil microbial communities that contribute to the spread of soil-borne diseases. Moreover, it offers possible biocontrol strains that might boost plant resilience to root rot. It's worth noting that these biocontrol strains showed signs of boosting plant development as well.

Supplementary Materials: The following supporting information can be downloaded at: https://www.mdpi.com/article/10.3390/f14081561/s1, Figure S1: Construction of Phylogenetic Tree by Combining Multiple Genes of HJGFB-1 strain. Phylogenetic tree inferred from the combined datasets (ITS, TEF, TUB, and RBP2) from members of the *F. solani* species analyzed. The evolutionary history was inferred by using the Bayesian Inference (BI) analyses, using *Fusarium plagianthi* NRRL22632 and *Fusarium vinguliforme* NRRL 32392 as the outgroup taxon.

Author Contributions: Methodology, Z.Z. and Y.L.; Data curation, S.H. and Z.Z.; Writing—original draft, Z.Z.; Writing—review & editing, Z.Z., S.H. and T.L.; Supervision, S.L. (Shujiang Li), S.L. (Shuying Li), C.Y. and T.Q.; Project administration, S.H. and T.Z. All authors have read and agreed to the published version of the manuscript.

Funding: This research was funded by the General Program of Science and Technology Department of Sichuan, Grant number 2019YFN0156.

Data Availability Statement: Not applicable.

Acknowledgments: Shan Han thanks the General Program of Science and Technology Department of Sichuan (Grant No. 2019YFN0156) for financial support.

Conflicts of Interest: The authors declare no conflict of interest.

References

1. Xu, D.; Zhuo, Z.; Wang, R.; Ye, M.; Pu, B. Modeling the Distribution of *Zanthoxylum armatum* in China with MaxEnt Modeling. *Glob. Ecol. Conserv.* **2019**, *19*, e00691.
2. Dušan, K.; Branka, L. Modern Trends in the Development of Agriculture and Demands on Plant Breeding and Soil Management. *Genetika* **2012**, *44*, 201–216.
3. Cao, Z.M.; Tian, C.M.; Liang, Y. Investigation on Zanthoxylum Prickly Ash Diseases in Shaanxi and Gansu Provinces. *J. Northwest For. Univ.* **1994**, *9*, 39–43. (In Chinese)
4. Niu, B.; Wang, W.; Yuan, Z.; Sederoff, R.R.; Sederoff, H.; Chiang, V.L.; Borriss, R. Microbial Interactions Within Multiple-Strain Biological Control Agents Impact Soil-Borne Plant Disease. *Front. Microbiol.* **2020**, *11*, 585404.
5. Fira, D.; Dimkić, I.; Berić, T.; Lozo, J.; Stanković, S. Biological Control of Plant Pathogens by *Bacillus* Species. *J. Biotechnol.* **2018**, *285*, 44–55.
6. Urbina, H.; Breed, M.F.; Zhao, W.; Gurrala, K.L.; Rosling, A. Specificity in *Arabidopsis thaliana* Recruitment of Root Fungal Communities from Soil and Rhizosphere. *Fungal Biol.* **2018**, *122*, 231.
7. Sanguin, H.; Sarniguet, A.; Gazengel, K.; Moenne-Loccoz, Y.; Grundmann, G.L. Rhizosphere Bacterial Communities Associated with Disease Suppressiveness Stages of Take-All Decline in Wheat Monoculture. *New Phytol.* **2019**, *184*, 694–707.
8. Rashid, M.I.; Mujawar, L.H.; Shahzad, T.; Almeelbi, T.; Ismail, I.M.I.; Oves, M. Bacteria and Fungi Can Contribute to Nutrients Bioavailability and Aggregate Formation in Degraded Soils. *Microbiol. Res.* **2016**, *183*, 26–41.
9. Arici, S.E.; Demirtas, A.E. The Effectiveness of Rhizosphere Microorganisms to Control Verticillium Wilt Disease Caused by *Verticillium dahliae* Kleb. in Olives. *Arab. J. Geosci.* **2019**, *12*, 781. [CrossRef]
10. Kennedy, A.C.; Smith, K.L. Soil Microbial Diversity and the Sustainability of Agricultural Soils. *Plant Soil* **1995**, *170*, 75–86.
11. Luo, L.; Guo, C.; Wang, L.; Zhang, J.; Deng, L.; Luo, K.; Huang, H.; Huang, H.; Liu, Y.; Liu, Y.; et al. Negative Plant-Soil Feedback Driven by Re-Assemblage of the Rhizosphere Microbiome with the Growth of *Panax notoginseng*. *Front. Microbiol.* **2019**, *10*, 1597. [CrossRef]
12. Wang, R.; Zhang, H.; Sun, L.; Qi, G.; Chen, S.; Zhao, X. Microbial Community Composition Is Related to Soil Biological and Chemical Properties and Bacterial Wilt Outbreak. *Sci. Rep.* **2017**, *7*, 343. [CrossRef]
13. Zhou, X.; Wu, F. Dynamics of the Diversity of Fungal and Fusarium Communities during Continuous Cropping of Cucumber in the Greenhouse. *FEMS Microbiol. Ecol.* **2012**, *80*, 469–478. [CrossRef]
14. Cha, J.Y.; Han, S.; Hong, H.J.; Cho, H.; Kim, D.; Kwon, Y.; Kwon, S.K.; Crüsemann, M.; Bok Lee, Y.; Kim, J.F.; et al. Microbial and Biochemical Basis of a Fusarium Wilt-Suppressive Soil. *ISME J.* **2016**, *10*, 119–129. [CrossRef]
15. Li, H.; Ma, X.; Tang, Y.; Yan, C.; Hu, X.; Huang, X.; Lin, M.; Liu, Z. Integrated Analysis Reveals an Association between the Rhizosphere Microbiome and Root Rot of *Arecanut palm*. *Pedosphere* **2021**, *31*, 725–735. [CrossRef]
16. Pieterse, C.M.; Zamioudis, C.; Berendsen, R.L.; Weller, D.M.; Van Wees, S.C.; Bakker, P.A. Induced Systemic Resistance by Beneficial Microbes. *Annu. Rev. Phytopathol.* **2014**, *52*, 347–375. [CrossRef]
17. Vandenkoornhuyse, P.; Quaiser, A.; Duhamel, M.; Le Van, A.; Dufresne, A. The Importance of the Microbiome of the Plant Holobiont. *New Phytol.* **2015**, *206*, 1196–1206. [CrossRef]
18. Islam, M.A.; Nain, Z.; Alam, M.K.; Banu, N.A.; Islam, M.R. In Vitro Study of Biocontrol Potential of Rhizospheric *Pseudomonas aeruginosa* against *Fusarium oxysporum* f. sp. Cucumerinum. *Egypt. J. Biol. Pest Control* **2018**, *28*, 90. [CrossRef]
19. Álvarez, B.; Biosca, E.G. Bacteriophage-Based Bacterial Wilt Biocontrol for an Environmentally Sustainable Agriculture. *Front. Plant Sci.* **2017**, *8*, 1218. [CrossRef]
20. Cazorla, F.M.; Mercado-Blanco, J. Biological Control of Tree and Woody Plant Diseases: An Impossible Task? *BioControl* **2016**, *61*, 233–242.
21. Yuan, J.; Chaparro, J.M.; Manter, D.K.; Zhang, R.; Vivanco, J.M.; Shen, Q. Roots from distinct plant developmental stages are capable of rapidly selecting their own microbiome without the influence of environmental and soil edaphic factors. *Soil Biol. Biochem.* **2015**, *89*, 206–209.
22. Frey-Klett, P.; Burlinson, P.; Deveau, A.; Barret, M.; Tarkka, M.; Sarniguet, A. Bacterial-Fungal Interactions: Hyphens between Agricultural, Clinical, Environmental, and Food Microbiologists. *Microbiol. Mol. Biol. Rev.* **2011**, *75*, 583–609.
23. Hassani, M.A.; Durán, P.; Hacquard, S. Microbial Interactions within the Plant Holobiont. *Microbiome* **2018**, *6*, 58.
24. Kemen, E. Microbe–Microbe Interactions Determine Oomycete and Fungal Host Colonization. *Curr. Opin. Plant Biol.* **2014**, *20*, 75–81. [CrossRef]

25. Hong, Y.; Chen, S.; Zhang, Y.; Chen, Y.; Yu, L.; Liu, Y.; Liu, Y.; Cheng, H.; Liu, Y. Rapid Identification of Soil Organic Matter Level via Visible and Near-Infrared Spectroscopy: Effects of Two-Dimensional Correlation Coefficient and Extreme Learning Machine. *Sci. Total Environ.* **2018**, *644*, 1232–1243.
26. Bremner, J.M. Determination of Nitrogen in Soil by the Kjeldahl Method. *J. Agric. Sci.* **1960**, *55*, 11–33.
27. Qiao, J.; Zhu, Y.; Jia, X.; Huang, L.; Shao, M. Vertical Distribution of Soil Total Nitrogen and Soil Total Phosphorus in the Critical Zone on the Loess Plateau, China. *Catena* **2018**, *166*, 310–316.
28. Zebec, V.; Rastija, D.; Lončarić, Z.; Bensa, A.; Popović, B.; Ivezić, V. Comparison of Chemical Extraction Methods for Determination of Soil Potassium in Different Soil Types. *Eurasian Soil Sci.* **2017**, *50*, 1420–1427. [CrossRef]
29. Fang, Z.D. *Plant Disease Research Methods*, 3rd ed.; China Agricultural Press: Beijing, China, 1998.
30. Schuck, S.; Weinhold, A.; Luu, V.T.; Baldwin, I.T. Isolating Fungal Pathogens from a Dynamic Disease Outbreak in a Native Plant Population to Establish Plant-Pathogen Bioassays for the Ecological Model Plant Nicotiana Attenuata. *PLoS ONE* **2014**, *9*, e102915.
31. O'Donnell, K. Progress towards a Phylogenetic Classification of Fusarium. *Sydowia* **1996**, *48*, 57–70.
32. Wu, X.; Zhang, H.; Chen, J.; Shang, S.; Wei, Q.; Yan, J.; Tu, X. Comparison of the Fecal Microbiota of Dholes High-Throughput Illumina Sequencing of the V3–V4 Region of the 16S RRNA Gene. *Appl. Microbiol. Biotechnol.* **2016**, *100*, 3577–3586. [CrossRef]
33. Xiong, W.; Zhao, Q.; Xue, C.; Xun, W.; Zhao, J.; Li, R.; Wu, H. Comparison of Fungal Community in Black Pepper-Vanilla and Vanilla Monoculture Systems Associated with Vanilla *Fusarium* Wilt Disease. *Front. Microbiol.* **2016**, *7*, 117. [CrossRef]
34. Liu, S.; Li, P.; Van Zwieten, L.; Tu, J.; Gan, W.; Lu, S.; Wang, H.; Wu, L. Edaphic Variables Influence Soil Bacterial Structure under Successive Fertilization of *Paulownia* Plantation Substituting Native Vegetation. *J. Soils Sediments* **2021**, *21*, 2922–2937. [CrossRef]
35. Lin, T.; Li, L.; Gu, X.; Owusu, A.M.; Li, S.; Han, S.; Cao, G.; Zhu, T.; Li, S. Seasonal Variations in the Composition and Diversity of Rhizosphere Soil Microbiome of Bamboo Plants as Infected by Soil-Borne Pathogen and Screening of Associated Antagonistic Strains. *Ind. Crop. Prod.* **2023**, *197*, 116641. [CrossRef]
36. Edgar, R.C. UPARSE: Highly Accurate OTU Sequences from Microbial Amplicon Reads. *Nat. Methods* **2013**, *10*, 996–998. [CrossRef] [PubMed]
37. Caporaso, J.G.; Kuczynski, J.; Stombaugh, J.; Bittinger, K.; Bushman, F.D.; Costello, E.K.; Fierer, N.; Peña, A.G.; Goodrich, J.K.; Gordon, J.I.; et al. QIIME Allows Analysis of High-Throughput Community Sequencing Data. *Nat. Methods* **2010**, *7*, 335–336. [CrossRef] [PubMed]
38. Lin, T.; Lu, Q.; Zheng, Z.; Li, S.; Li, S.; Liu, Y.; Zhu, T.; Chen, L.; Yang, C.; Han, S. Soil cadmium stress affects the phyllosphere microbiome and associated pathogen resistance differently in male and female poplars. *J. Exp. Bot.* **2023**, *74*, 2188–2202. [CrossRef] [PubMed]
39. Sunar, K.; Chakraborty, U.; Chakraborty, B.N. Exploitation of Native Microflora of Darjeeling Hills for Sclerotial Rot Management and Growth Promotion in Pulses. *Indian Phytopathol.* **2014**, *67*, 59–69.
40. Ritpitakphong, U.; Falquet, L.; Vimoltust, A.; Berger, A.; Métraux, J.P.; L'Haridon, F. The microbiome of the leaf surface of Arabidopsis protects against a fungal pathogen. *New Phytol.* **2016**, *210*, 1033–1043.
41. Masum, M.M.I.; Liu, L.; Yang, M.; Hossain, M.M.; Siddiqa, M.M.; Supty, M.E.; Ogunyemi, S.O.; Hossain, A.; An, Q.; Li, B. Halotolerant Bacteria Belonging to Operational Group *Bacillus amyloliquefaciens* in Biocontrol of the Rice Brown Stripe Pathogen Acidovorax Oryzae. *J. Appl. Microbiol.* **2018**, *125*, 1852–1867. [CrossRef]
42. Borba, M.P.; Ferrero, A.P.D.S.; de Souza Lameira, R.; Van Der Sand, S.T. The Intricate Molecular Identification of Streptomyces: A Case Study on Antarctic Soil Isolates. *Arch. Microbiol.* **2022**, *204*, 476. [CrossRef] [PubMed]
43. Dixon, P. VEGAN, a Package of R Functions for Community Ecology. *J. Veg. Sci.* **2003**, *14*, 927–930. [CrossRef]
44. Ginestet, C. ggplot2: Elegant Graphics for Data Analysis. *J. R. Stat. Soc. Ser. A Stat. Soc.* **2011**, *174*, 245–246. [CrossRef]
45. Robinson, M.D.; McCarthy, D.J.; Smyth, G.K. EdgeR: A Bioconductor Package for Differential Expression Analysis of Digital Gene Expression Data. *Bioinformatics* **2010**, *26*, 139–140. [CrossRef]
46. Langille, M.G.I.; Zaneveld, J.; Caporaso, J.G.; McDonald, D.; Knights, D.; Reyes, J.A.; Clemente, J.C.; Burkepile, D.E.; Vega Thurber, R.L.; Knight, R. Predictive Functional Profiling of Microbial Communities Using 16S RRNA Marker Gene Sequences. *Nat. Biotechnol.* **2013**, *31*, 814–821. [CrossRef]
47. Qu, Q.; Zhang, Z.; Peijnenburg, W.J.G.M.; Liu, W.; Lu, T.; Hu, B.; Chen, J.; Chen, J.; Lin, Z.; Qian, H. Rhizosphere Microbiome Assembly and Its Impact on Plant Growth. *J. Agric. Food Chem.* **2020**, *68*, 5024–5038. [CrossRef]
48. Luan, F.G.; Zhang, L.L.; Lou, Y.Y.; Wang, L.; Liu, Y.N.; Zhang, H.Y. Analysis of Microbial Diversity and Niche in Rhizosphere Soil of Healthy and Diseased Cotton at the Flowering Stage in Southern Xinjiang. *Genet. Mol. Res.* **2015**, *14*, 1602–1611. [CrossRef]
49. Van Elsas, J.D.; Chiurazzi, M.; Mallon, C.A.; Elhottovā, D.; Krištůfek, V.; Salles, J.F. Microbial Diversity Determines the Invasion of Soil by a Bacterial Pathogen. *Proc. Natl. Acad. Sci. USA* **2012**, *109*, 1159–1164. [CrossRef]
50. Raza, W.; Ling, N.; Zhang, R.; Huang, Q.; Xu, Y.; Shen, Q. Success Evaluation of the Biological Control of Fusarium Wilts of Cucumber, Banana, and Tomato since 2000 and Future Research Strategies. *Crit. Rev. Biotechnol.* **2016**, *26*, 202–212. [CrossRef] [PubMed]
51. Egamberdieva, D. *Bacillus* Spp.: A Potential Plant Growth Stimulator and Biocontrol Agent under Hostile Environmental Conditions. In *Bacilli and Agrobiotechnology*; Springer: Cham, Switzerland, 2016; pp. 91–111.
52. Lee, S.; Gi, K.H.; Cheol, S.G.; Min, R.C. Disruption of Firmicutes and Actinobacteria Abundance in Tomato Rhizosphere Causes the Incidence of Bacterial Wilt Disease. *ISME J.* **2020**, *15*, 330–347. [CrossRef]

53. Rosenzweig, N.; Tiedje, J.M.; Quensen, J.F., III; Meng, Q.; Hao, J.J. Microbial Communities Associated with Potato Common Scab-Suppressive Soil Determined by Pyrosequencing Analyses. *Plant Dis.* **2012**, *96*, 718–725. [CrossRef] [PubMed]
54. Fan, B. *Bacillus velezensis* FZB42 in 2018: The Gram-Positive Model Strain for Plant Growth Promotion and Biocontrol. *Front. Microbiol.* **2018**, *9*, 2491. [CrossRef] [PubMed]
55. Paul, C.S.; Anton, H.; Gao, X.W.; Rainer, B. Biocontrol Mechanism by Root-Associated *Bacillus amyloliquefaciens* FZB42—A Review. *Front. Microbiol.* **2015**, *6*, 780.